Arabian Journal of Chemistry (2015) xxx, xxx–xxx

King Saud University

Arabian Journal of Chemistry

www.ksu.edu.sa
www.sciencedirect.com

ORIGINAL ARTICLE

Characterization of a sensitive biosensor based on an unmodified DNA and gold nanoparticle composite and its application in diquat determination

Ling Mei Niu [a], Ying Liu [b], Kao Qi Lian [a], Li Ma [a], Wei Jun Kang [a,c,*]

[a] School of Public Health, Hebei Medical University, Shijiazhuang 050017, China
[b] Tangshan Gongren Hospital, Tangshan 063000, China
[c] Key Laboratory of Forensic Medicine of Hebei Province, Shijiazhuang 050017, China

Received 31 October 2014; accepted 13 March 2015

KEYWORDS

CA DNA;
Gold nanoparticles;
Diquat;
Gold electrode

Abstract DNA usually adsorbs gold nanoparticles by virtue of mercapto or amino groups at one end of a DNA molecule. However, in this paper, we report a sensitive biosensor constructed using unmodified DNA molecules with consecutive adenines (CA DNA) and gold nanoparticles (GNPs). The CA DNA–GNP composite was fabricated on gold electrodes and characterized by using of scanning electron microscopy (SEM), electrochemical impedance spectroscopy (EIS) and the electrochemical method. Using an electrochemical quartz crystal microbalance (EQCM), the mechanism by which the CA DNA and GNPs combined was also studied. The modified electrode exhibited an ultrasensitive response to diquat. Differential pulse voltammetry (DPV) was used to study the linear relationships between concentrations and reduction peak currents, ranging from 1.0×10^{-9} M to 1.2×10^{-6} M. The detection limit of it is 2.0×10^{-10} M. The feasibility of the proposed assay for use in human urine and grain was investigated, and the satisfactory results were obtained.

1. Introduction

Diquat (1,1′-dimethyl-4, 4′-bipyridilium dibromide) is one of the most widely used herbicides, and holds the largest share of the global herbicide market until recently overtaken by glyphosate (Mhammedi et al., 2009). However, DQ possesses undesirable characteristics those are highly toxic to human health, the repeated exposures may cause skin irritation, sensitization, or ulcerations on contact (Vanholder et al., 1981).

* Corresponding author at: School of Public Health, Hebei Medical University, Shijiazhuang, 050017, China. Tel./fax: +86 31186265754.
E-mail address: kangwj158@hebmu.edu.cn (W.J. Kang).

Peer review under responsibility of King Saud University.

Production and hosting by Elsevier

http://dx.doi.org/10.1016/j.arabjc.2015.03.009
1878-5352

With a remarkable persistence in the environment, DQ represents a potential danger to the natural waters due to its high solubility (about 620 g L^{-1} at 25 °C) (Bethesda, 1988). From above, whether the DQ can be accurately quantified in samples has become important. Therefore, there is an increasing need for rapid reliable method to measure DQ concentrations in the real samples.

Nowadays, a numerous of analytical techniques have been applied for the analysis of DQ, such as fluorescence (Pérez-Ruiz et al., 1991; Carrillo-Carrión et al., 2011), chromatography (Shōzi et al., 1984; Cherukury et al., 1995) and chromatography/mass spectrometry (Rafael and Mauricio, 2007; Hao et al., 2013). Although chromatography is a conventional method, it often requires a concentration step to improve the detection limits, resulting in sample destruction (Walcarius and Lamberts, 1996). Moreover, other methods are comparatively complicated and require expensive equipments, highly qualified technicians and specialized laboratories. By contrast, electrochemistry is an interesting and convenient alternative that simplifies detection processes and enhances the response signals of the analytes (Walcarius and Lamberts, 1996).

In recent years, the development of DNA biosensor has received much attention because of its extreme importance in numerous fields. As is well known, the immobilization of DNA onto electrode surfaces is one of the key steps toward DNA sensor development (Zhang et al., 2010). Usually, by virtue of the mercapto or amino groups at one end of DNA molecules, they can be anchored on gold nanoparticles (GNPs) because GNPs have large specific surface area, high surface free energy, better biocompatibility, and suitability for constructing DNA biosensors (Zhang et al., 2010; Lin et al., 2010). Nevertheless, some of the deficiencies for this strategic assembly are the imprecise controls of the orientation and conformation of surface-tethered DNA. In addition, the coulomb and electromagnetic interactions between nanoparticles are prominent effects on the distribution of GNPs (Yao and Yaomura, 2013). Thus, investigating a new fabrication strategy to better control the interaction forces between GNPs and finding a new method to assemble DNAs are necessary.

The study on the affinity of DNA for combining with GNPs revealed that the four nucleotides display high affinities, whereas adenine interacts much more strongly with the gold surface compared with the other nucleotides (Storhoff et al., 2002). Fan and co-workers demonstrated that the affinities of consecutive adenines (CA, which means continuous arrangement of adenine bases,) were even comparable to the strength of an Au−S chemical bond. Furthermore, the DNA monolayer fabricated with CA blocks (CA DNA) showed better order and the upright conformation of it increased advantages in target DNA hybridization or detection (Pei et al., 2012). In addition, the method offers a more cost-effective alternative, considering that the thiol or amino fabrications can be >90% of the total cost of DNA synthesis (for example, $0.30/bp for gene synthesis while $50 for DNA modification for Sangon Biotech Co., Ltd.) (Zhang et al., 2012).

Our previous report has presented a biosensor constructed by three-dimensional (3D) GNPs and studied the simultaneous determination of dopamine, uric acid, adenine and guanine (Niu et al., 2013). However, the 3D GNPs were constructed by unmodified double-strand DNA (ds-DNA) and the lesser exposure of bases and the rigid structure of ds-DNA make them exhibit less interaction with GNPs (An and Jin, 2012). This paper aimed to report a novel DNA fabrication method by virtue of the CA DNA. With the aid of CA blocks, CA DNAs could be fabricated on GNPs in a highly order and upright structure. The sensitivity of the presented biosensor was consequently improved. The electrostatic interactions between DQ and all of the CA DNAs, are the main reaction to interpret. The CA DNA–GNP composite was successfully applied in human urine and grain determination with satisfactory results.

2. Experimental

2.1. Reagents

4-Mercaptobenzoic acid, 4-aminothiophenol, N-(3-dimethyla minopropyl)-N′-ethylcarbodiimide hydrochloride (EDC) and DQ were purchased from Sigma. Hydrogen tetrachloroaurate (III) tetrahydrate ($HAuCl_4{\cdot}3H_2O$) and sodium citrate were obtained from the Sinopharm Chemical Reagent Co., Ltd. and were used as received.

Human urine samples were obtained from The Second Hospital of Hebei Medical University. Phosphate buffer solutions (PBS, 0.1 M) of different pH values were prepared by mixing stock solutions of 0.1 M KH_2PO_4 and 0.1 M Na_2HPO_4 (Shanghai Chemical Reagent Company). The pH was adjusted using 0.1 M H_3PO_4 or NaOH (Shanghai Chemical Reagent Company). Citrate buffer (0.01 M, pH 3.0) was prepared by mixing 0.01 M citric acid and 0.01 M sodium citrate. $K_3Fe(CN)_6$ and KCl were also obtained from the Shanghai Chemical Reagent Company. All chemicals used were of analytical-reagent grade. Water (>18 MΩ cm) was obtained from a SMART ultra-pure water system.

Various oligonucleotides were purchased from the Shanghai Sangon Bioengineering Technology and Services Co., Ltd. The solutions (0.1 mM) were prepared with citrate buffer (pH 3.0) and stored at 4 °C. Their sequences were as follows:

Probe ss-DNA (1): 5′-AAA TAC GCC ACC AGC TCC-3′
Target ss-DNA (2): 5′-AAA GGA GCT GGT GGC GTA-3′

2.2. Apparatus

Electrochemical impedance spectroscopy (EIS) was performed on a CHI 650D and electrochemical experiments were carried out on a CHI 440 electrochemical workstation (Chen Hua Instruments Co., Shanghai, China) with a three-electrode system, which includes the working electrode, a platinum wire counter electrode, and an Ag/AgCl reference electrode. The electrochemical quartz crystal microbalance (EQCM) experiments were performed on a CHI 440 electrochemical workstation with a 7.995 MHz AT-cut quartz crystal. A polished Au/Cr-coated AT-cut quartz crystal was used as the working electrode. The reference and the counter electrodes were similar to those used in the electrochemical studies. All potentials were provided with respect to the Ag/AgCl electrode (saturated KCl).

The sizes of GNPs were measured using a transmission electron microscopy (TEM, HITACHI-600, HITACHI Co., Japan) and gold colloid concentration was determined with

Please cite this article in press as: Niu, L.M. et al., Characterization of a sensitive biosensor based on an unmodified DNA and gold nanoparticle composite and its application in diquat determination. Arabian Journal of Chemistry (2015), http://dx.doi.org/10.1016/j.arabjc.2015.03.009

UV–vis spectrophotometer (UV-7500, Keda Instrument Co. Ltd.). Scanning electron microscopy (SEM) images were obtained using a HITACHI S-4800 operated at 0 and 3 kV (HITACHI S-4800, HITACHI Co., Japan). A SMART ultra-pure water system (Heal Force SMART-N, Heal Force Development Ltd.) was also used. All experiments were carried out under the protection of high-purity nitrogen.

2.3. Thiol/GNP/CA DNA composite preparation

According to the references (Pei et al., 2012; Zhang et al., 2012), gold colloid solution of 13 nm dimension was selected in the following research. Gold colloid solutions were prepared according to the method of Frens (1973) with slight modifications. Briefly, All of the glasswares were thoroughly cleaned with freshly prepared nitro-hydrochloric acid (1:3; HNO_3:HCl). 50.0 mL of 0.2 g L^{-1} $HAuCl_4$ was brought to a rolling boil with vigorous stirring in a 100 mL round-bottom flask. The rapid addition of 4.0 mL of 10 g L^{-1} sodium citrate to the vortex of the solution resulted in a color change from pale yellow to orange red. Boiling was continued for 15 min, the heating mantle was then removed, and stirring was continued until the solution reached room temperature. The resulting solution of colloidal particles was characterized by an absorption maximum at 520 nm. The concentration of gold colloid is 6.78×10^{-9} M.

The gold electrode (GE) surface was mechanically polished with slurries of alumina (0.3 and 0.05 μm diameter successively) and washed ultrasonically in fresh Piranha solution (H_2SO_4: H_2O_2 = 3: 1 (v/v)), absolute ethanol, and water for 10 min, respectively. Then, it was electrochemically cleaned in 1.0 M H_2SO_4 by potential scanning between 0 and 1.7 V until a reproducible cyclic voltammogram (CV) was obtained. Finally, the gold electrode was dried under nitrogen flow until further use.

Because the short backbone of dithiol compound offers only a weak intermolecular stabilization, it will lead to a reclined molecular orientation after adsorption on gold substrate (Waqas et al., 2011). Thus, in order to form a well-ordered, self-assembled monolayer, fabrication of GNP anchoring matrix was carried out in two steps. First, the bare electrode was soaked in 4-mercaptobenzoic acid solution (0.01 M in ethanol) for 12 h. Second, the electrode was immersed in 4-aminothiophenol solution (0.01 M in ethanol) in the presence of 5 mM EDC for 12 h at room temperature (Li et al., 2008). Using EDC as a crosslinking agent, carboxyl group of 4-mercaptobenzoic acid could covalent combine with amino group of 4-aminothiophenol. Then, the thiols-modified electrode was transferred into gold colloid solution of 13 nm for 12 h at 4 °C (thiol/GNP composite). After hybridizing of probe ss-DNA (1) with target ss-DNA (2) in advance at 47 °C for 1 h to prepare crosslinking DNA solution, the GNP modified electrode was then incubated in the above solution for 2 h (*thiol/GNP/CA DNA* composite) (Lin et al., 2011).

The fabrication of the GNP–CA DNA modified electrode is illustrated in Scheme 1.

3. Results and discussion

3.1. Characteristics of GE/thiol/GNP/CA DNA

To confirm each modification process of the electrode, electrochemical methods, SEM, EIS and electrochemical methods are performed. Fig. 1A illustrates the image of bare gold electrode on AT-cut quartz crystal. Ordered GNPs are shown in Fig. 1B after anchoring on the thiol monolayer. Then, only a small quantity of GNPs could be observed (Fig. 1C). That maybe because the CA DNA molecules were almost adsorbed on GNPs by consecutive adenines after rinsing in the CA DNA solution, and DNA cannot be observed well by SEM. So, it seemed that the quantity of GNP decreased. Fig. 1D is the TEM morphology of 13 nm gold colloid and inset of it is the photograph of gold colloid solution. The approximate quantity of CA DNA on each GNP was calculated in the subsequent research. Because of the well order of CA DNA molecules, there is a series of triangles were formed between GNPs (as shown in Scheme 1). This structure is not only believable to decrease the effects caused by coulomb and electromagnetic interactions between GNPs, but also a favorable factor to improve the stability and orderliness of GNPs.

Changes of the impedance on the electrode surface in the modification process can be determined through EIS. Thus, EIS was also used to evaluate the interfacial electron-transfer efficiency at different stages of biosensor preparation (Lin et al., 2010). In this work, impedance measurements were performed at frequencies ranging from 0.01 Hz to 10^6 Hz and with formal potential of 0.14 V in a solution containing 0.1 M KCl, 5.0 mM $[Fe(CN)_6]^{3-}/[Fe(CN)_6]^{4-}$, and 0.1 M phosphate buffer solution (PBS) at a pH of 7.0. A small semicircle can be observed in the Nyquist plot of the bare GCE, as shown in Fig. 2 (curve a). Its electron transfer resistance (R_{et}) is 2.6 kΩ. The interfacial R_{et} corresponding to the semicircle diameters gradually increased from 2.6 kΩ to 11.3 kΩ (for the 4-mercaptobenzoic acid monolayer, curve b) and 18.7 kΩ (for the thiol (4-mercaptobenzoic acid and 4-aminothiophenol) monolayer, curve c) because the thiols monolayer perturbed the interfacial electron transfer rates between the electrode and the electrolyte solution. In the next step, electron transfer occurs more easily because the nanometer-sized GNPs act as conducting wires or electron-conducting tunnels (Szymanska et al., 2007). Thus, the R_{et} obviously decreased (R_{et} = 3.8 kΩ) after nano-Au absorption on the electrode surface (curve d). The increased R_{et} (R_{et} = 13.7 kΩ, the discrepancy of 9.9 kΩ) observed after the CA DNA immobilization could be ascribed to the repellence of negatively charged DNA phosphate skeletons (curve e).

The electron transfer behaviors after each modification step of thiols, GNPs, CA DNAs were investigated by cyclic voltammetry in $[Fe(CN)_6]^{3-}$ solution (as shown in Fig. 3). The bare gold electrode (GE) exhibited well-defined current responses for $[Fe(CN)_6]^{3-}$, indicating a diffusion-controlled electron transfer on the bare GE (black curve) (Souza and Machado, 2005). Then, the current responses decreased because of the poor conductions of the thiols covering on the GE (red curve). However, the GNPs anchored on the modified electrode greatly increased the current responses of the redox couples (green curve). This result shows that the GNPs perhaps act as nanoscale electrodes ensemble, which make it easier for the efficient electron transfer through their conducting tunnels. After the CA DNAs being anchored on the modified electrode, the current responses for the redox couples decreased again due to the repulsions between the negatively charged DNA backbones and ferricyanides (blue curve).

Please cite this article in press as: Niu, L.M. et al., Characterization of a sensitive biosensor based on an unmodified DNA and gold nanoparticle composite and its application in diquat determination. Arabian Journal of Chemistry (2015), http://dx.doi.org/10.1016/j.arabjc.2015.03.009

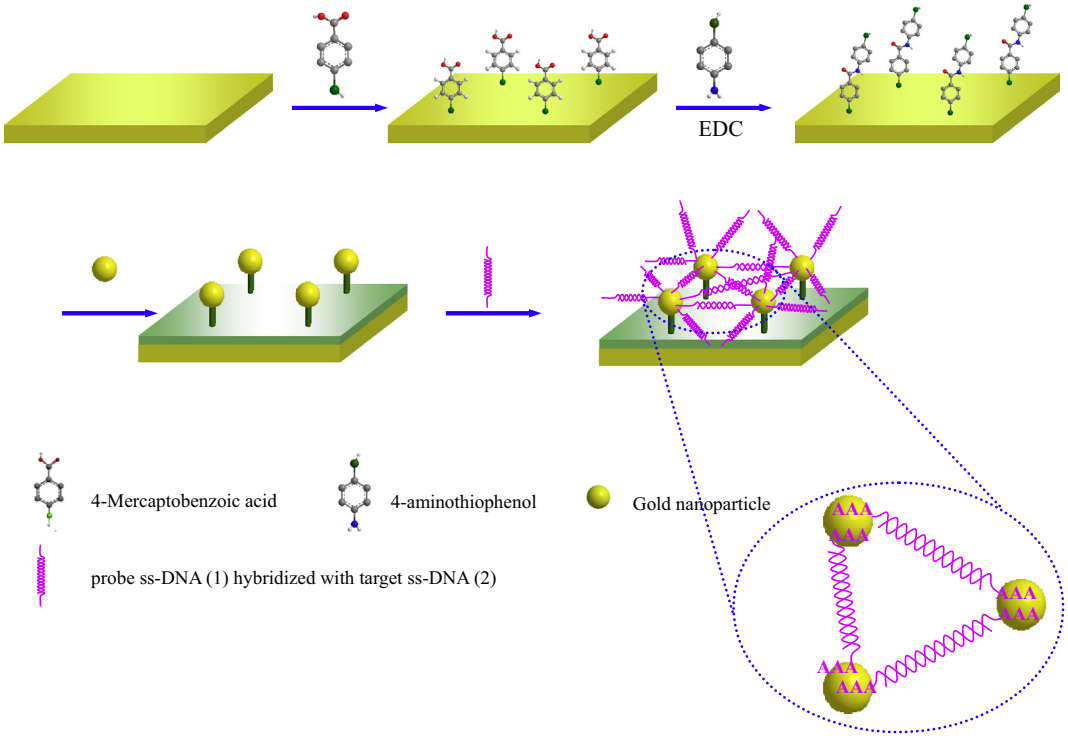

Scheme 1 Modification of the CA DNA and GNP composite.

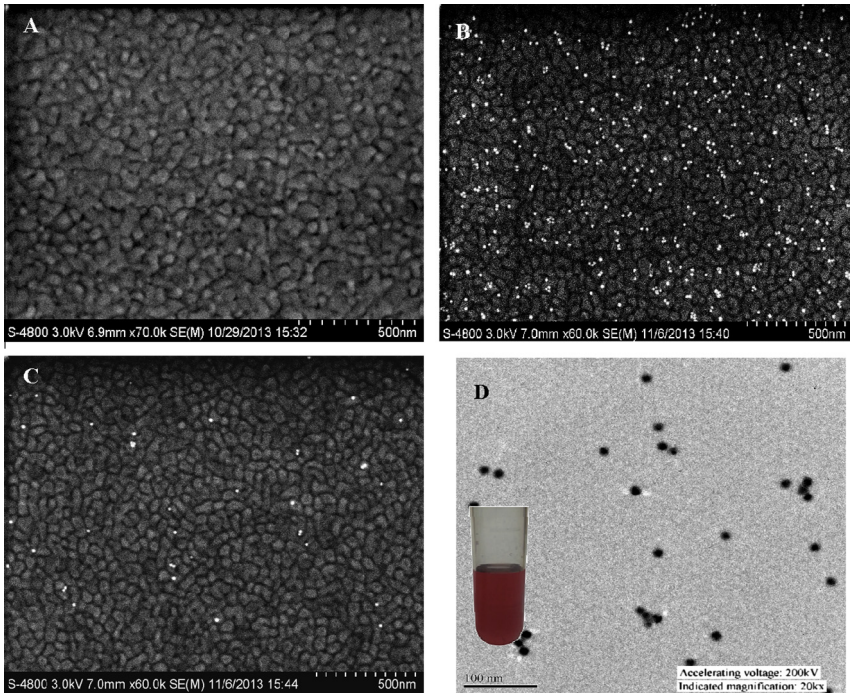

Figure 1 SEM morphology of (A) bare gold electrode, (B) GE/thiol/GNP, (C) GE/thiol/GNP/CA DNA and TEM morphology of GNP (D). Inset is the photograph of gold colloid solution.

3.2. Mechanism by which the CA DNA and GNPs combine

The EQCM is a variant of acoustic wave microsensors that are capable of ultra-sensitive mass measurements. For an 8 MHz crystal, the mass change is 1.34 ng for 1 Hz frequency change. The experiment relies on the calculation of mass change (ΔM) at the quartz crystal using the measured frequency change (Δf) (Sauerbrey equation) (Ock et al., 2002):

$$\Delta f = -2F_0^2 \Delta M / \left[A(\mu\rho)^{1/2}\right] \quad (1)$$

Please cite this article in press as: Niu, L.M. et al., Characterization of a sensitive biosensor based on an unmodified DNA and gold nanoparticle composite and its application in diquat determination. Arabian Journal of Chemistry (2015), http://dx.doi.org/10.1016/j.arabjc.2015.03.009

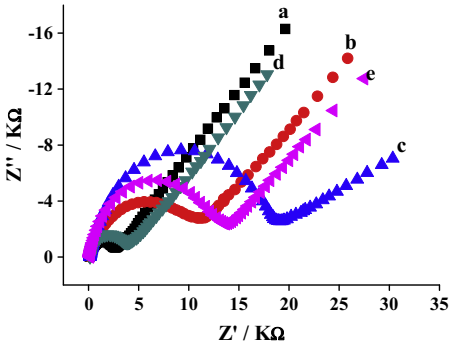

Figure 2 Complex impedance plots measured in 5.0 mM $Fe(CN)_6^{3-}/Fe(CN)_6^{4-}$ + 0.1 M KCl+ phosphate buffer (pH 7.0) at formal potential of 0.24 V for (a) bare gold electrode, (b) 4-mercaptobenzoic acid-modified electrode, (c) thiol (4-mercaptobenzoic acid and 4-aminothiophenol)-modified electrode, (d) GE/thiol/GNP, and (e) GE/thiol/GNP/CA DNA. The frequency range is between 10^{-2} and 10^{6} Hz with signal amplitude of 50 mV.

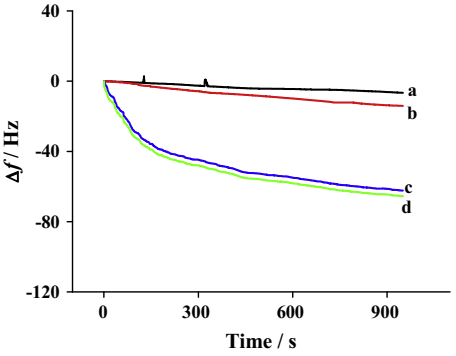

Figure 4 Frequency responses of the electrode at different modification steps. (a) Bare gold electrode, (b) thiols (4-mercaptobenzoic acid and 4-aminothiophenol) modified electrode, (c) GE/thiol/GNP, and (d) GE/thiol/GNP/CA DNA.

where F_0 is the fundamental resonant frequency (7.995 MHz), ΔM (g) is the mass gain, A is the electrode area (0.196 cm^2), ρ is the density of the quartz (2.684 g cm^{-3}), and μ is the shear module (2.947×10^{10} g cm^{-1} s^2). By using the EQCM, the conjugation between CA DNA and GNPs was studied. As Fig. 4 shows, the frequency of bare electrode (Fig. 4a) was almost unchanged (at 0 Hz). A slightly changed mass of the electrode was observed after the thiols modification (Fig. 4b). But the electrode mass dramatic rose after fabrication of the GNPs (Fig. 4c). Similarly, the continuous frequency decrease exhibited mass increment on the electrode after the modification by CA DNAs (Fig. 4d). The frequency declined for GNPs and CA DNAs by 55 and 3.2 Hz, respectively. Accordingly, the mass changes were 74 ng for GNPs and 4.3 ng for CA DNAs, respectively. Meanwhile, if the mass of each GNP is known, the quantity of CA DNA adsorbed on each GNP can be obtained.

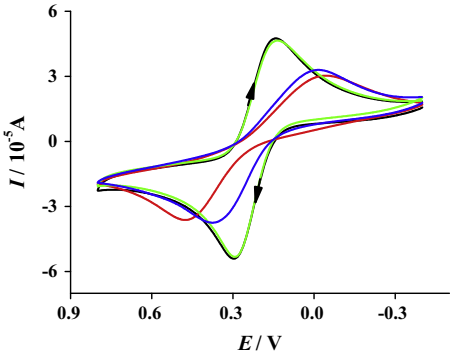

Figure 3 Cyclic voltammograms of 5.0×10^{-3} M $Fe(CN)_6^{3-}$ on a bare gold electrode (black curve) and each step of surface modification of gold electrode (GE) with thiols (red curve), GNP monolayer (green curve), CA DNA layer (blue curve) using 1 M KCl and a scan rate of 0.1 V s^{-1}. (For interpretation of the references to colour in this figure legend, the reader is referred to the web version of this article.)

The concentration of gold colloid can be acquired according to the following equation (2):

$$Abs = \varepsilon bC \quad (2)$$

where Abs is the absorbance of gold colloid solution, which is 1.83 at 520 nm; ε is the extinction coefficient, which is 2.7×10^8 M^{-1} cm^{-1} at λ = 520 nm for 13 nm particles (Wang et al., 2008); and b is the path length of the spectrometer, which is usually 1 cm. Then, the C of gold colloid is calculated as a value of 6.78×10^{-9} M. Based on the mass of gold in $HAuCl_4$ solution and molar mass of CA DNA, the quantity of CA DNA adsorbed on each GNP is approximately 100, which is similar with the data presented in a previous report (Zhang et al., 2012).

3.3. Electrochemical behaviors of DQ at the GE/thiol/GNP/CA DNA

The reductive responses of DQ on the electrode at each fabrication step were investigated by differential pulse voltammetry (DPV) (Fig. 5). As Fig. 5 shows, there were no peaks in the absence of DQ on the modified electrode (curve a). Usually, the electroreduction of DQ is regarded as a two-step process. Correspondingly, two reductive peaks were observed. The potential of them are about −0.25 V and −0.55 V, respectively. Because the second peak showed better linear relationship to the concentration of DQ, the second reductive peak was selected as the quantitative peak of DQ. From Fig. 5, only small peaks of DQ were observed on the bare electrode (curve b). The reductive peak current and peak potential of the second peak are 7.04×10^{-7} A and −0.552 V, respectively. Low peaks of DQ can be observed on the thiol-modified electrode because of the affinity between thiols and DQ (curve c) (Tatsuya and Daisuke, 2002). The thiol monolayer provides a template on which to anchor GNPs, generating a 2-dimensional (2D) array of GNP modified electrode. The better response of DQ on the GNP modified electrode than on the thiols monolayer could be ascribed to the large surface area of GNPs, which accelerated the electron transfer (curve d) (Karolina et al., 2009). However, remarkable increases of current responses were observed on the CA DNA-modified electrode (curve e) because of the electrostatic interactions between the negatively charged backbones of DNA and

Please cite this article in press as: Niu, L.M. et al., Characterization of a sensitive biosensor based on an unmodified DNA and gold nanoparticle composite and its application in diquat determination. Arabian Journal of Chemistry (2015), http://dx.doi.org/10.1016/j.arabjc.2015.03.009

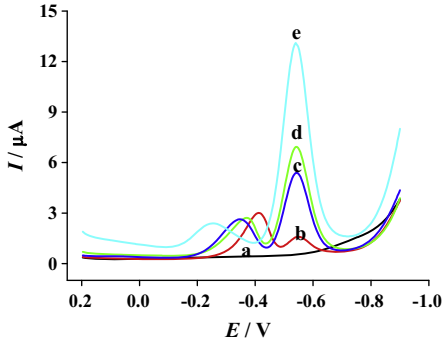

Figure 5 DPVs recorded using (b) bare electrode, (c) thiol (4-mercaptobenzoic acid and 4-aminothiophenol)-modified electrode, (d) GE/thiol/GNP, (e) GE/thiol/GNP/CA DNA in the absence (a) and presence (b–e) of DQ.

positively charged DQs. The peak current and potential of the second peak are 1.17×10^{-5} A and −0.54 V, respectively. Consequently, relative to those on the bare electrode, the currents of the second reductive peak were magnified 17-fold. The better response and the higher reductive potential on modified electrode indicated that the GNP/CA DNA composite exhibited much better sensitivity.

3.4. Determination of DQ on GE/thiol/GNP/CA DNA

The effect of pH on the electrochemical response of 1.0×10^{-7} M DQ on the modified electrode was investigated in phosphate buffer solution (PBS) using DPV. Based on the second reduction peak, which can be seen in Fig. 6, the peak currents increased with increasing pH until pH 8.0, and then gradually decreased. This can be explained by the fact that at low pH, there are more proton ions competing with DQ on the modified electrode. Thus, an increasing pH is favorable for improving the response of DQ on the modified electrode. However, just as paraquat, DQ is stable in acidic or neutral solutions but hydrolyzes in alkaline solutions, the peak currents did not climb up steadily but reached their maximum of pH 8.0, then decreased. Considering the determination sensitivity, the pH value of 8.0 was chosen as the optimal pH condition and used in the succeeding experiments.

After optimization of the voltammetric conditions, calibration curves were obtained by DPV (Fig. 7) on the modified electrode. The relationships between peak currents around

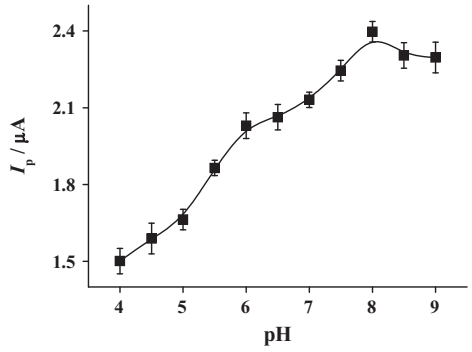

Figure 6 Effect of pH on DQ determination. DQ concentration: 1.0×10^{-7} M.

−0.54 V and their concentrations were investigated. Under the optimal conditions, the peak currents at −0.54 V had good linear relationships with the DQ concentrations ranging from 1.0×10^{-9} M to 1.2×10^{-6} M. The detection limit was 2.0×10^{-10} M (signal to noise ratio: 3). The linear regression equation is $I_p = 0.1953 + 20.6833C$ (I_p: μA, C: μM, r: 0.9983). The calibration plots of peak currents versus DQ concentrations are shown in the insets. The results indicated that the proposed assay method showed an ultrasensitive response because of the well-ordered CA DNAs fabricated GNPs. Compared with other presented methods, this CA DNA/GNP composite exhibited lower detection limit, higher sensitivity, and better selectivity. A comparison of detection limits and linear ranges between the proposed assay and other methods is shown in Table S1.

3.5. Reproducibility and stability of GE/thiol/GNP/CA DNA

A series of repetitive measurements were conducted in the solution containing 3.0×10^{-7} M DQ to evaluate the precision and stability of the modified electrode. The average relative standard deviation of 20 successive determinations of DQ was 2.4%, demonstrating an excellent reproducibility. The storage stability of the modified electrode was also investigated in 0.1 M PBS (pH 7.0) at 4 °C on different days. After 3 months, a current response of approximately 98% of the original value could still be observed. Thus, the proposed electrode stability is sufficiently effective for continuous operation.

3.6. Interference

The selectivity was studied by DPV and the tolerance limit was taken as the maximum concentration of foreign substances that causes approximately ±5% relative error in determination. First, possible interferences for the selective determination of DQ in urine were investigated by the addition of foreign species into a DQ solution of 7.0×10^{-7} M. The tolerated ratios of foreign substances were 1:3000 for Na^+, K^+, Ca^{2+}, Mg^{2+}, Zn^{2+}, Fe^{3+}, Cl^-, SO_4^{2-}, CO_3^{2-}, and PO_4^{3-}; 1:50 for lysine, glucose, lactic acid, dopamine and ascorbic

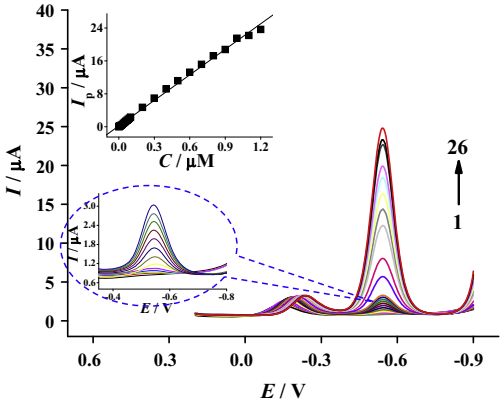

Figure 7 DPVs of DQ at the modified electrode in 0.1 M PBS (pH: 8.0). Inset is the calibration plots of DQ. DQ concentrations (from 1 to 26, 10^{-7} M): 0.01, 0.03, 0.05, 0.07, 0.09, 0.1, 0.2, 0.3, 0.4, 0.5, 0.6, 0.7, 0.8, 0.9, 1.0, 2.0, 3.0, 4.0, 5.0, 6.0, 7.0, 8.0, 9.0, 10, 11, 12.

Please cite this article in press as: Niu, L.M. et al., Characterization of a sensitive biosensor based on an unmodified DNA and gold nanoparticle composite and its application in diquat determination. Arabian Journal of Chemistry (2015), http://dx.doi.org/10.1016/j.arabjc.2015.03.009

acid; and 1:30 for glutamic acid, l-cystine and uric acid. The interference concentrations and DQ recovery are presented in Table S2. The recovery of DQ is between 95.3% and 102%, which is evident that the modified electrode shows an excellent selectivity toward these species.

3.7. Real-life sample analysis

The practical application of the electrode modified with CA DNA–GNP composite was tested by DPV. The proposed method was applied for the DQ detection of human urine and grain. Urine samples of DQ from intoxation patients were frozen until determination and diluted to 1:1000. Grain of 5.0 g was taken and rinsed in 100.0 ml water by ultrasonication for 10 min before running on the workstation. All the samples were spiked with appropriate amounts of DQ. The results are shown in Table S3. The high recoveries of the spiked DQ demonstrated a good accuracy and reliability of the proposed method.

4. Conclusions

The results obtained in this paper demonstrated that unmodified DNA with CA block exhibited a better orderliness and sensitivity toward DQ determination. The electrode modified with CA DNA–GNP composite showed well-defined curves in the electrochemical process of DQ by DPV. The proposed method exhibited a higher sensitivity and a lower detection limit compared with other reported methods. This method was successfully applied in the determination of DQ in human urine and grain. Thus, the method presented in the current work is promising in clinical diagnoses and analytical researches.

Acknowledgments

The authors are deeply grateful to the National Natural Science Foundation of China (Nos. 81402720), the foundations of Health and Family Planning commission of Hebei (20130460), Key Lab of Analytical Science Technology of Hebei (AST-1403) and Hebei Food and Drug Administration (Pt2014044)for the support they extended.

Appendix A. Supplementary material

Supplementary data associated with this article can be found, in the online version, at http://dx.doi.org/10.1016/j.arabjc.2015.03.009.

References

An, H.J., Jin, B., 2012. Biotechnol. Adv. 30, 1721.
Bethesda, M.D., 1988. Hazardous Substances Databank. National Library of Medicine, U.S..
Carrillo-Carrión, C., Bartolomé, M.S., Miguel, V., 2011. Anal. Chim. Acta 692, 103.
Cherukury, M., Zoltan, G., Klaassen, C.D., 1995. J. Chromatogr. B 674, 193.
Frens, G., 1973. Nat. Phys. Sci. 241, 20.
Hao, C.Y., Zhao, X.M., David, M., Yang, P., Taguchi, V., Franca, M., 2013. J. Chromatogr. A 1304, 169.
Karolina, C., Andreas, O., Dirk, M., 2009. Phys. Stat. Solidi (A) 206, 489.
Li, N.B., Park, J.H., Park, K., Kwon, S.J., Shin, H., Kwak, J., 2008. Biosens. Bioelectron. 23, 1519.
Lin, L.Q., Chen, J., Lin, Q.H., Chen, W., Chen, J.H., Yao, H., Liu, A.L., Lin, X.H., Chen, Y.Z., 2010. Talanta 80, 2113.
Lin, L.Q., Liu, Q.C., Wang, L.M., Liu, A.L., Weng, S.H., Lei, Y., Chen, W., Lin, X.H., Chen, Y.Z., 2011. Biosens. Bioelectron. 28, 277.
Mhammedi, M.A.E., Bakasse, M., Najih, R., Chtaini, A., 2009. Appl. Clay Sci. 43, 130.
Niu, L.M., Lian, K.Q., Shi, H.M., Wu, Y.B., Kang, W.J., Bi, S.Y., 2013. Sensor. Actuators B: Chem. 178, 10.
Ock, J.Y., Shin, H.K., Kwon, Y.S., 2002. Inter. J. Nanosci. 1, 593.
Pei, H., Li, F., Wan, Y., Wei, M., Liu, H.J., Su, Y., Chen, N., Huang, Q., Fan, C.H., 2012. J. Am. Chem. Soc. 134, 11876.
Pérez-Ruiz, T., Martínez-Lozano, C., Tomás, V., 1991. Anal. Chim. Acta 244, 99.
Rafael, M.A., Mauricio, Y., 2007. J. Chromatogr. B 853, 260.
Shōzi, K., Susumu, K., Shigeo, U., 1984. J. Chromatogr. A 283, 231.
Souza, D.D., Machado, S.A.S., 2005. Anal. Chim. Acta 546, 85.
Storhoff, J.J., Elghanian, R., Mirkin, C.A., Letsinger, R.L., 2002. Langmuir 18, 6666.
Szymanska, I., Radecka, H., Radecki, J., Kaliszan, R., 2007. Biosens. Bioelectron. 22, 1955.
Tatsuya, N., Daisuke, N., 2002. Tetrahedron Lett. 43, 5719.
Vanholder, R., Colardyn, F., DeReuck, J., Praet, M., Lameire, N., Ringoir, S., 1981. Am. J. Med. 70, 1267.
Walcarius, A., Lamberts, L., 1996. J. Electroanal. Chem. 406, 59.
Wang, H., Wang, Y.X., Jin, J.Y., Yang, R.H., 2008. Anal. Chem. 80, 9021.
Waqas, K., Mira, E.H., Tobias, M., 2011. ACS Nano 5, 9870.
Yao, H., Yaomura, S., 2013. Langmuir 29, 6444.
Zhang, X., Liu, B.W., Dave, N., Servos, M.R., Liu, J.W., 2012. Langmuir 28, 17053.
Zhang, Y.Z., Wang, J., Xu, M.L., 2010. Colloids Surf. B 75, 179.